Обзор ArXiv:astro-ph, 13-17 июля 2020

От Сильченко О.К.

ArXiv: 2007.07824

ALMA resolves the remarkable molecular jet and rotating wind in the extremely radio-quiet galaxy NGC 1377

S. Aalto[1], N. Falstad[1], S. Muller[1], K. Wada[2], J. S. Gallagher[3], S. König[1], K. Sakamoto[4], W. Vlemmings[1], C. Ceccobello[1], K. Dasyra[5], F. Combes[6], S. García-Burillo[7], Y. Oya[10], S. Martín[8,9], P. van der Werf[11], A. S. Evans[12], and J. Kotilainen[13]

(Affiliations can be found after the references)

Received xx; accepted xx

ABSTRACT

Submillimetre and millimetre line and continuum observations are important in probing the morphology, column density, and dynamics of the molecular gas and dust around obscured active galactic nuclei (AGNs) and their mechanical feedback. With very high-resolution (0.″02 × 0.″03 (2 × 3 pc)) ALMA 345 GHz observations of CO 3–2, HCO^+ 4–3, vibrationally excited HCN 4–3 v_2=1f, and continuum we have studied the remarkable, extremely radio-quiet, molecular jet and wind of the lenticular galaxy NGC 1377. The outflow structure is resolved, revealing a 150 pc long, clumpy, high-velocity (~600 km s^{-1}), collimated molecular jet where the molecular emission is emerging from the spine of the jet with an average diameter of 3-7 pc. The jet widens to 10-15 pc about 25 pc from the centre, which is possibly due to jet-wind interactions. A narrow-angle (50°-70°), misaligned and rotating molecular wind surrounds the jet, and both are enveloped by a larger-scale CO-emitting structure at near-systemic velocity. The jet and narrow wind have steep radial gas excitation gradients and appear turbulent with high gas dispersion (σ>40 km s^{-1}). The jet shows velocity reversals that we propose are caused by precession, or more episodic directional changes. We discuss the mechanisms powering the outflow, and we find that an important process for the molecular jet and narrow wind is likely magneto-centrifugal driving. In contrast, the large-scale CO-envelope may be a slow wind, or cocoon that stems from jet-wind interactions. An asymmetric, nuclear r~2 pc dust structure with a high inferred molecular column density $N(H_2) \simeq 1.8 \times 10^{24}$cm^{-2} is detected in continuum and also shows compact

Небольшие S0-галактики… BUT LIRGи!

NGC 1377

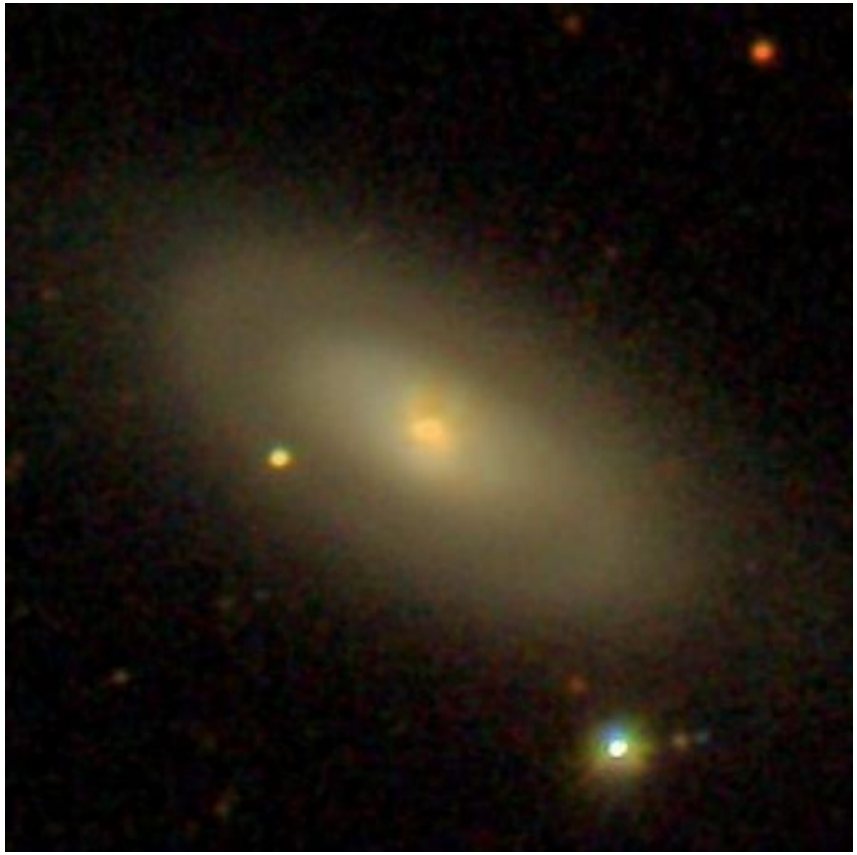

NGC 4418

V_los>80km/s

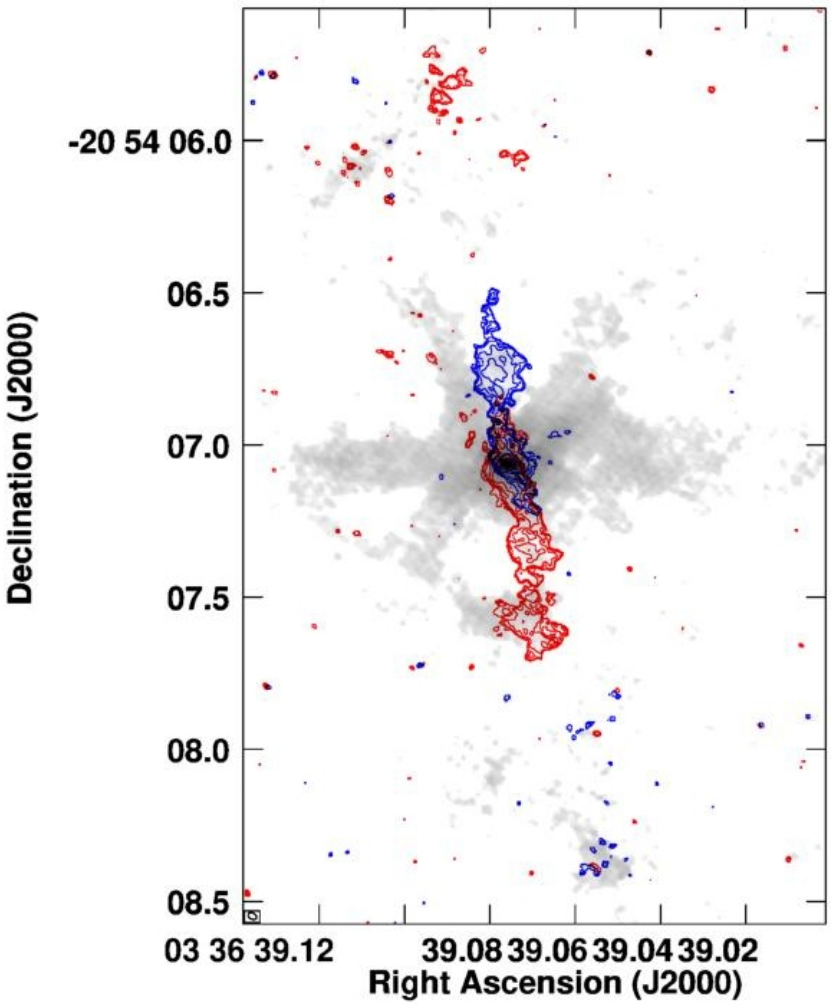

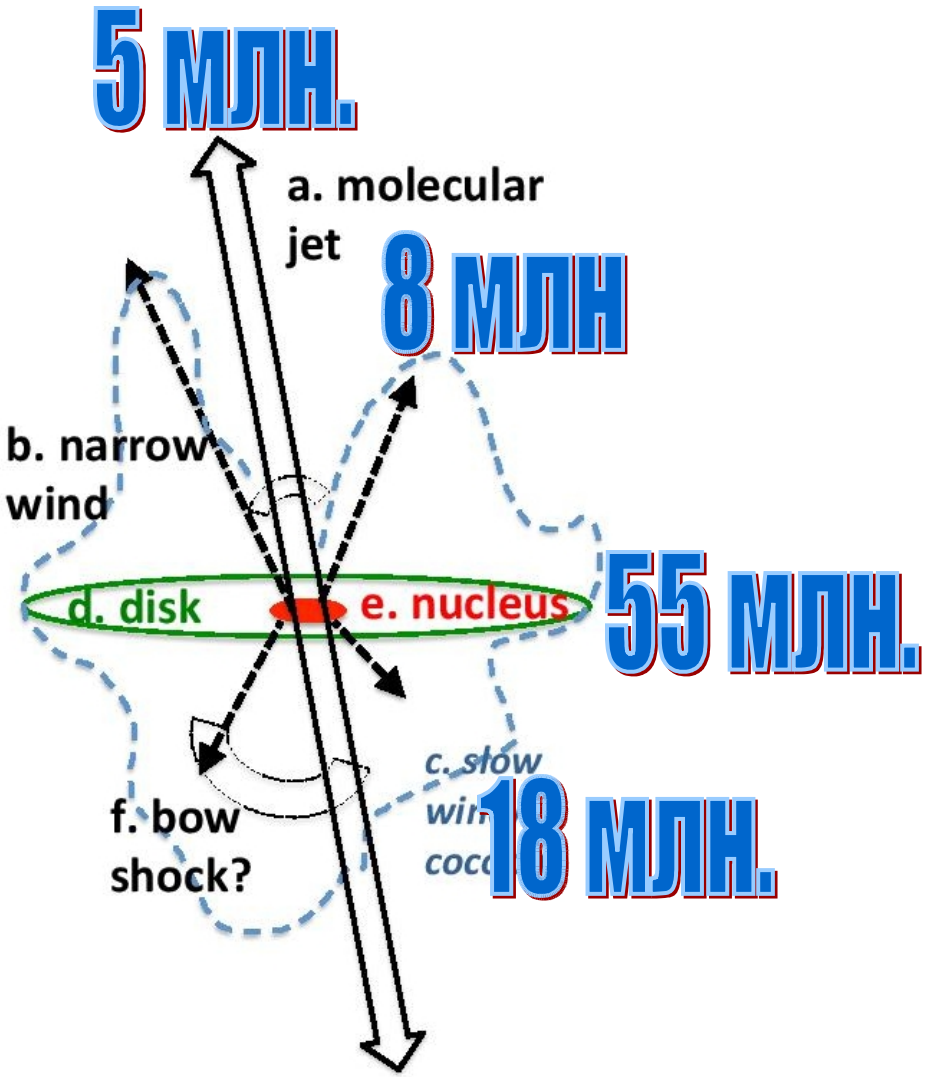

5 млн.

8 млн

55 млн.

18 млн.

солнечных масс молекулярного газа!

Полный диапазон скоростей CO(3→2)

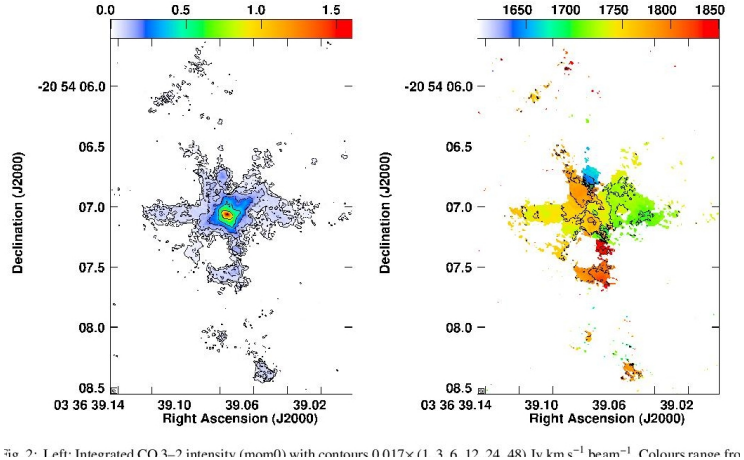

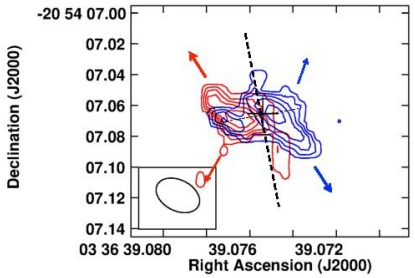

Fig. 4: Red- and blueshifted high-velocity gas: Nuclear orientation of rotation (Blue: 1552 - 1572 km s^{-1}; Red: 1886 - 1906 km s^{-1}). (Contours 0.004×(1,2,3,4,5) Jy beam^{-1} kms^{-1}). The thick, black, and dashed line indicates the jet orientation, the thin line the orientation of the nuclear velocity shift. The red and blue arrows indicate the narrow wind.

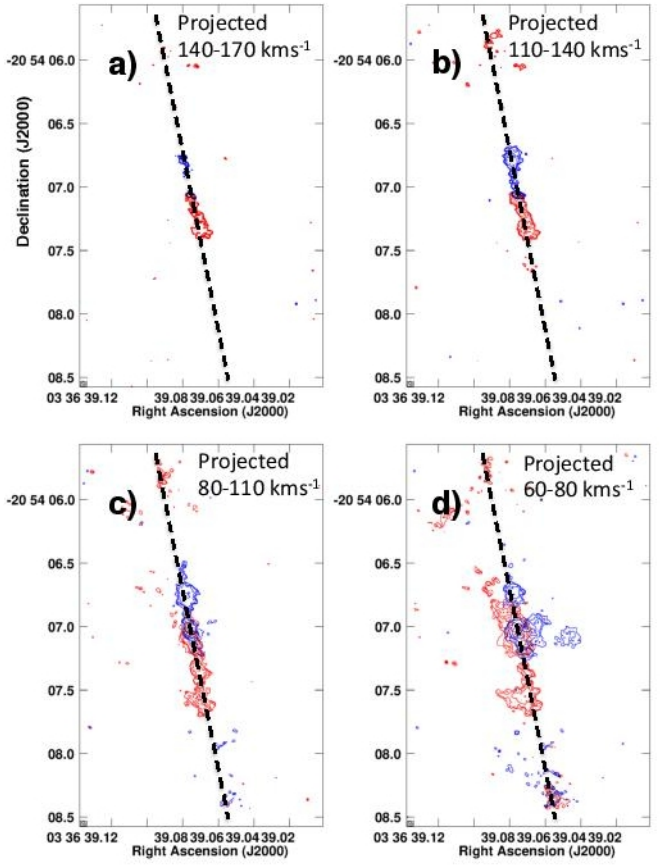

Fig. 5: Panels showing the structure of the jet at various ve
locity intervals: Top left panel: Highest velocity, projected ve

совсем ядро

HCO+: центральный диск, до 3пк

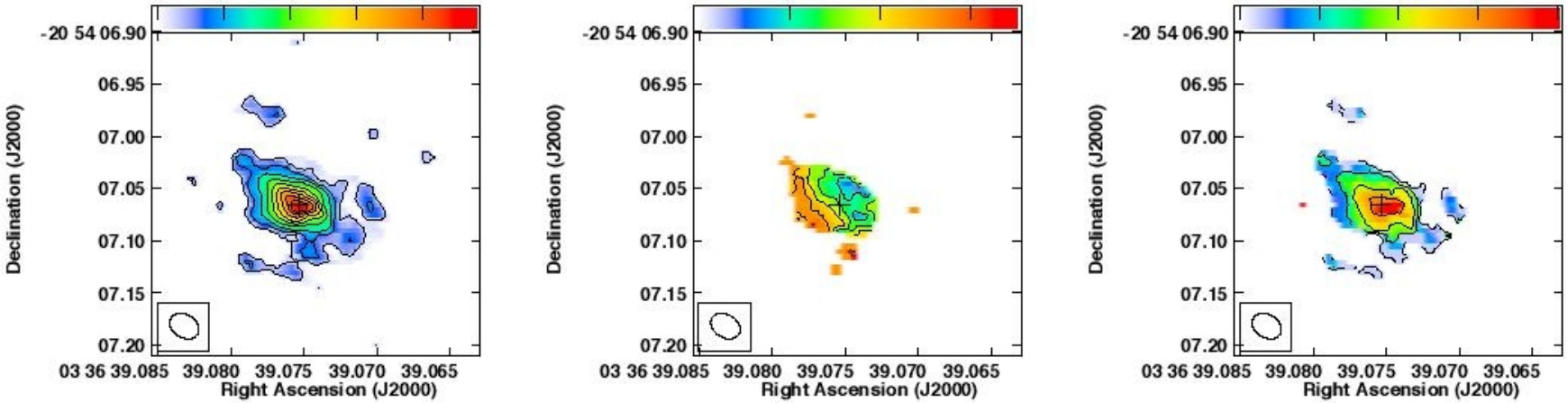

Fig. 6: HCO^+ 4–3 moment maps. Left: Integrated intensity (mom0) where contours are 0.025× (1, 3,5,7,9,11,13,15,17) Jy km s^{-1} $beam^{-1}$. Colours range from 0 to 0.48 Jy km s^{-1} $beam^{-1}$. Centre: velocity field (mom1) where contours range from 1650km s^{-1} to 1825 km s^{-1} in steps of 25 km s^{-1}, colours range from 1650 to 1825 km s^{-1}. Right: Dispersion map (mom2) where contours are 10×(2,4,6,8) km s^{-1}. Colours range from 20 to 100 km s^{-1}. The cross indicates the position of the 345 GHz continuum peak.

Бюджет структур

Table 2: Kinetic and gravitational energy

Component	Velocity ($km\,s^{-1}$)	σ ($km\,s^{-1}$)	K^a	W^a
Jet	600	30-60	11.2	0.01
NW	90	30	0.4	0.03
SW/C	30	10	0.2	0.03
Disk	27	10-30	0.3	0.80
BH				0.03
Stars				17
Total[b]			~12	~18

[a] The kinetic energy is $K \simeq \frac{1}{2} M(v^2 + \sigma^2)$ where M is the mass of the component (jet, NW=narrow wind, SW/C=slow wind (also the envelope or cocoon), disk), v its velocity and σ its dispersion. In units of $\times 10^{11}$ $M_\odot$ $(pc/Myr)^2$. For the SW/C we assume an average outflow velocity of 30 $km\,s^{-1}$. The rotational velocity of the disk is assuming an i=70°. The gravitational energy is $W \simeq G\frac{M^2}{r}$ where M is the mass of the component. Units are 10^{11} $M_\odot$ $(pc/Myr)^2$. W_{BH} is the gravitational energy of the central SMBH inside r_{env}=100 pc and W_{star} is that of the stellar and envelope system for the same region. The mass of the stars inside r=100 pc is estimated to 2×10^8 $M_\odot$ from an HST H-band image (HST program GO14728, J Gallagher PI).

[b] The total kinetic energy of the system $K_{total}=K_{jet}+K_{wind}+K_{disk}$ and the total gravitational energy of the system $W_{total}=W_{jet}$ + W_{cm} + W_{disk} + W_{BH} + W_{star} out to a radius r=100 pc.

ArXiv: 2007.07905

Constraints on the star formation histories of galaxies in the Local Cosmological Volume

P. Kroupa,[1,2]* M. Haslbauer,[1] I. Banik,[1]† S.T. Nagesh,[3] and J. Pflamm-Altenburg[1]
[1] *Helmholtz-Institut für Strahlen- und Kernphysik, Universität Bonn, Nussallee 14-16, 53115 Bonn, Germany*
[2] *Charles University in Prague, Faculty of Mathematics and Physics, Astronomical Institute, V Holešovičkách 2, CZ-180 00 Praha, Czech Republic*
[3] *Argelander-Institut für Astronomie, Auf dem Hügel 71, 53121 Bonn, Germany*

17 July 2020

ABSTRACT
The majority of galaxies with current star-formation rates (SFRs), $SFR_{\rm o} \geqslant 10^{-3}\,M_\odot/{\rm yr}$, in the Local Cosmological Volume where observations should be reliable, have the property that their observed $SFR_{\rm o}$ is larger than their average star formation rate. This is in tension with the evolution of galaxies described by delayed-τ models, according to which the opposite would be expected. The tension is apparent in that local galaxies imply the star formation timescale $\tau \approx 6.7$ Gyr, much longer than the $3.5-4.5$ Gyr obtained using an empirically determined main sequence at several redshifts. Using models where the SFR is a power law in time of the form $\propto (t-t_1)^\eta$ for $t_1 = 1.8$ Gyr (with no stars forming prior to t_1) implies that $\eta = 0.18 \pm 0.03$.

Выборка

The Catalogue of Neighbouring Galaxies (Karachentsev et al. 2004) and its update (Karachentsev et al. 2013) are used to extract the K-band luminosities and the SFRs based on integrated Hα and far ultraviolet (FUV) measurements for galaxies within a distance of ≈ 11 Mpc. The catalogue also lists limit flags on the FUV- and Hα-based SFR values. If a SFR value is marked with such a flag, it is excluded from the here presented analysis (but including flagged SFR values does not significantly affect the results). This gives a sample of 870 galaxies, from 1145. From these 870 galaxies, 267 have only far ultraviolet (FUV)-based SFR values, 128 have only Hα based SFRs, and 475 have both measurements available. Thus, 14.7% and 30.7% galaxies lack FUV- and Hα-based SFR measurements, respectively.[1] The K-band luminosity values are converted to M_* using a mass-to-light ratio of 0.6 (Lelli et al. 2016).

For galaxies which have both SFR measurements available, $SFR_{\rm o} = (SFR_{\rm FUV} + SFR_{\rm H\alpha})/2$ is adopted. Their SFRs based on integrated Hα and FUV measurements are depicted in Fig. 1. The condition $SFR_{\rm o} \geqslant 10^{-3}\,M_\odot/{\rm yr}$ leaves 386 galaxies. For the galaxies which only have the FUV- or Hα-based values, $SFR_{\rm o} = SFR_{\rm FUV}$ or $SFR_{\rm o} = SFR_{\rm H\alpha}$, respectively (these galaxies do not appear in Fig. 1). Applying the cut $SFR_{\rm o} \geqslant 10^{-3}\,M_\odot/{\rm yr}$ leaves 109 and 88 galaxies which have only $SFR_{\rm FUV}$ or $SFR_{\rm H\alpha}$ data, respectively.

С чем сравнивают:

- Speagle+ (2014)
- z=0-6, evolution of SF/MS
- Typically delayed exponential SFH, started 3 Gyr after BB, with exponential timescales of 3-4 Gyr

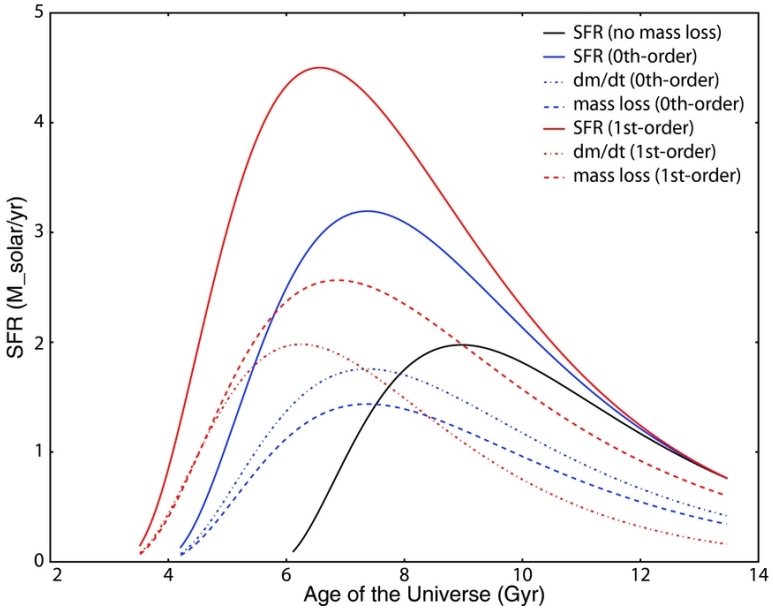

SFR~(t-t1)exp[-(t-t1)/tau]

max SFR: t-t1=tau

У галактик ближнего объема – постоянная SFR

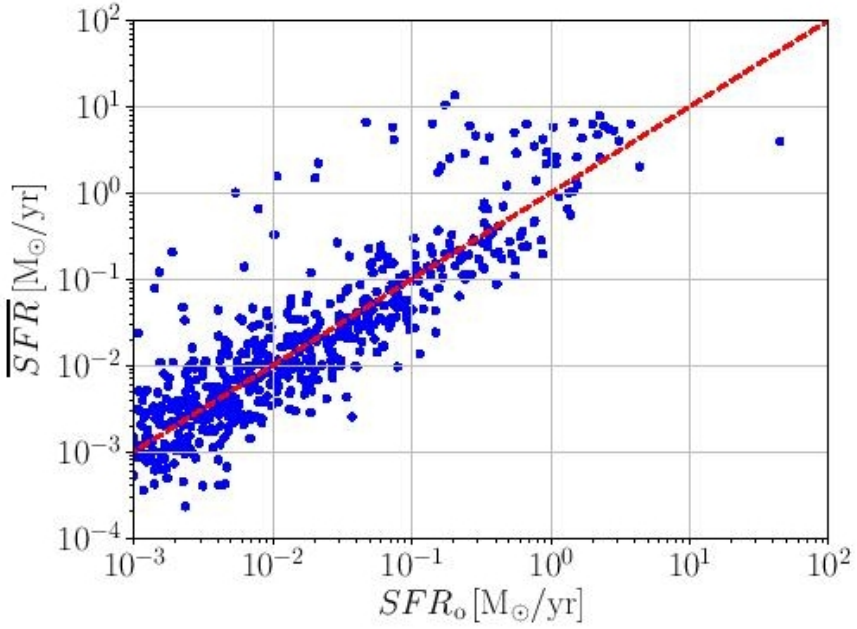

Figure 3. The present-day measured SFR, SFR_o, is compared with the average value, $\overline{SFR}$, for each galaxy (filled squares, Sec. 2) for galaxies with $SFR_o \geqslant 10^{-3}\,M_\odot$/yr and assuming $\zeta = 1.3, t_{sf} = 12\,$Gyr. The dashed line is the 1:1 relation. Note that the data suggest a second sequence of galaxies lying ≈ 2 dex above the ridge line populated by the majority of galaxies near the 1:1 line. This sequence is discussed further in Haslbauer et al. (in prep.) and may be related to galaxies which have lost their inter-stellar medium being replenished through stellar evolutionary mass loss.

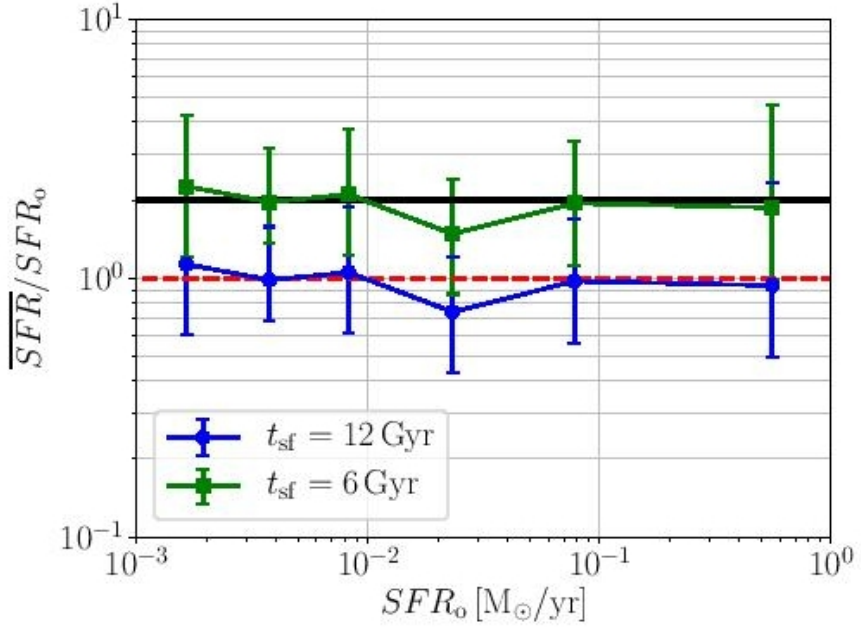

Figure 4. Using galaxies with $SFR_o \geqslant 10^{-3}\,M_\odot$/yr, the ratio between the average SFR and the present-day value is plotted in bins containing 100 galaxies (except for the right-most bin, which contains 83 galaxies) in order to test Eq. 1. The points and error bars show the median and first-third interquartile range, respectively. The blue (green) points (squares) are for $t_{sf} = 12\,(6)$ Gyr, with lower t_{sf} leading to higher $\overline{SFR}$. The solid black line depicts the expected value of 2 (Eq. 9), while the dashed red line shows a value of 1.

Или слабо-растущие SFH, или неправильная космология…

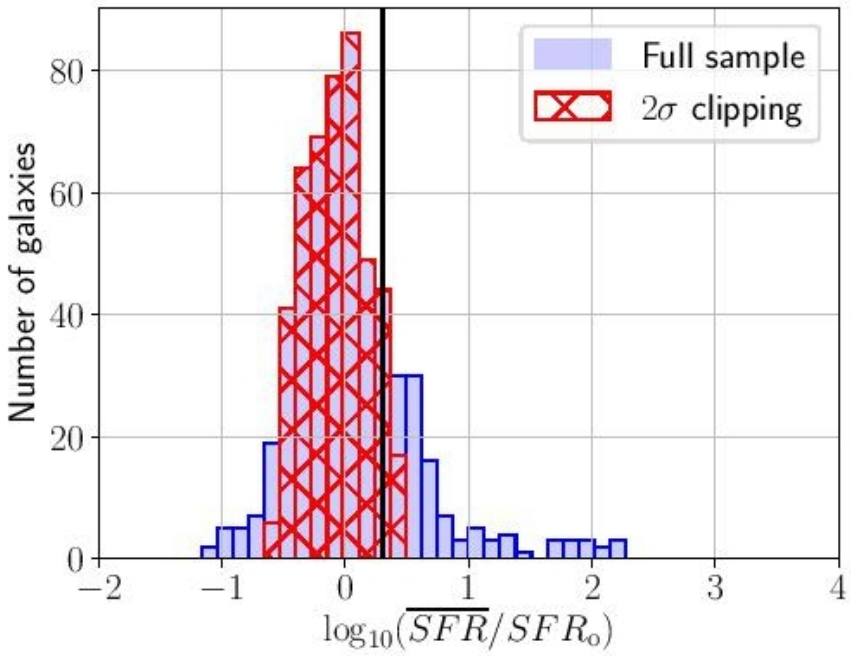

Figure 5. Histogram of $\overline{SFR}/SFR_{\rm o}$ values for galaxies with $SFR_{\rm o} \geqslant 10^{-3} M_{\odot}/{\rm yr}$ if $t_{\rm sf} = 12\,{\rm Gyr}$. The hatched red region shows the effect of 2σ outlier rejection, which reduces the sample size from 583 to 455. The $\overline{SFR}/SFR_{\rm o}$ values would double if $t_{\rm sf} = 6\,{\rm Gyr}$, so for clarity the expected horizontal shift is plotted as a vertical solid black line at $\log_{10} 2$. This is also the expected value according to the SFH obtained by SP14 (Eq. 9).